The effect of βFeOOH synthesis routes on its ability to corrode iron

Emmerson N. J.[1*], Watkinson D. E.[1], Roche K.[2], Seifert J. E.[1], Thunberg J. C.[1]

[1]*Cardiff University, Cardiff, UK*
[2]*Warren Lasch Conservation Center, Charleston, USA*

*Author for correspondence

Abstract

Akaganeite (βFeOOH) occludes chloride within its crystal structure and adsorbs it onto it surface during its formation. βFeOOH was synthesised by solid-state and aqueous precipitation routes. The amount of adsorbed chloride removed by a single aqueous wash was measured. The impact of the synthesised βFeOOH on the oxidation rate of iron was determined by using a remote oxygen sensing technique to record oxygen concentrations within a sealed vessel, internally controlled to 80% relative humidity and containing mixture of βFeOOH and iron powder. The oxidation rate of iron was directly related to the mass% of adsorbed chloride removed by the aqueous wash. This contributes to understanding of both iron corrosion and the development of conservation treatments.

Keywords

Iron; corrosion; archaeological; Akaganeite; chloride

Introduction

Conservation practitioners devise and apply treatments to fulfil perceived goals and require quantitative and qualitative research to evidence whether these are attained. The research design dictates the value of its outcomes to conservation practice and,

if this is flawed, it can foster misinterpretation and increase risk in conservation practice. Within any experimental design the sample introduces variables that impact on data quality, range, reproducibility and relevance to the question being addressed. While analogue samples can provide reproducibility, they are often problematic as they seek to replicate outcomes that may have taken years or centuries to achieve, such as reproducing patinas and corrosion product layers. In order to study corrosion or decay processes, research may require synthesis of compounds that are produced naturally on objects. While this often seems straightforward to achieve, questions remain regarding whether the synthesis routes produce similar chemistry and morphology to the compounds formed on objects, whether formation routes for analogues produce the same end product, how well an analogue represents contextual reality and, consequently, whether research results are transferable to conservation practice. This research considers these questions for the experimental use of synthesised βFeOOH to parallel the role of naturally formed βFeOOH in the corrosion and treatment of archaeological iron.

Archaeological iron: the corrosion problem

Chloride plays a major role in the post-excavation corrosion of archaeological iron. Turgoose's (1982a) corrosion model for buried archaeological iron reports Cl^- ions accumulating at the metal surface to provide charge balance for anodically generated Fe^{2+}. Above this, there is a dense corrosion product layer (DPL) that normally comprises a goethite, magnetite and maghemite matrix, overlaid by an altered porous layer of iron corrosion products and soil particles (Reguer et al. 2006; Neff et al. 2007). Localisation of chloride occurs at anodes on the metal, due to strips of magnetite that conduct electrons into the DPL where ingress of moisture and

oxygen support the cathode reaction (Neff et al. 2007). Highly mobile Cl^- ions from the soil pass through the corrosion matrix associating with Fe^{2+} ions at the anode. They can exist in solution and Reguer et al. (2006) identified the β-$Fe_2(OH)_3Cl$ iron hydroxy-chloride ferrous phase occurring next to the metal surface, postulating that it is a precursor for the formation of the oxidised ferric phase β-FeOOH (Akaganeite), which is detected above it. Turgoose (1982b) identified β-FeOOH on archaeological iron post-excavation, attributing it to oxidation of a Fe^{2+}/Cl^- solution at the metal surface by atmospheric oxygen and fresh oxidation of iron with chloride as an electrolyte. Oxidation generates more Fe^{2+} ions and their hydrolysis lowers pH in the thin moisture film which makes βFeOOH formation thermodynamically favourable in the prevailing high Cl^- ion concentration (Turgoose 1982b; Rémazeilles 2007).

βFeOOH occludes chloride in its crystal structure and adsorbs it onto its surface (Mackay 1962). The overall chloride content can vary but substantial amounts are often surface adsorbed. Reguer et al. (2009) produced βFeOOH with 12%mass chloride, attributing 6.7%mass of this to being within the crystal structure as determined by XRD structural analysis. They reduced chloride content to 4.5%mass after 10 washes in deionised water, which removed the adsorbed chloride and reduced the chloride in the crystal structure by 20%. The mobility of the adsorbed chloride in water and water vapour, make it readily available for corrosion of adjacent iron (Turgoose 1982b; Watkinson and Lewis 2005; Thickett and Odlyha 2013; Watkinson and Emmerson 2016). Lowering the amount of adsorbed chloride present on βFeOOH by aqueous washing treatments, reduces the extent and rate of corrosion it produces on iron (Watkinson and Emmerson 2016). While the residual

chloride in the crystal structure of βFeOOH is unavailable to support corrosion, it remains a risk if transformations occur and release it.

βFeOOH has been identified on archaeological objects (Thickett and Odlyha 2013) many times post-excavation and poses a major corrosion threat as it and any ferrous chloride present are hygroscopic, hence their corrosion threat is a function of prevailing relative humidity (RH) (Watkinson and Lewis 2005; Watkinson et al. 2019). For βFeOOH mixed with iron powder, corrosion ceases below 15% RH (Watkinson and Lewis 2005; Thickett and Odlyha 2013), and for ferrous chloride below 20% RH (Turgoose 1982b; Watkinson and Lewis 2005). For both compounds it is very slow below 30% RH then rises, finally escalating exponentially from 60% RH upwards (Watkinson and Lewis 2005; Watkinson et al. 2019). The prevalence and form of chloride will impact on its role and impact in corrosion processes, as will the access of moisture and oxygen to its location. Preventing its formation post-excavation is essential, since its growth at the metal surface cracks overlying corrosion product layers, which then spall off and hence destroy heritage value of an object.

Controlling corrosion of chloride infested iron

An obvious and proven option for non-interventive action to control corrosion is desiccation (Turgoose 1982b; Watkinson et al. 2019; Thunberg et al. 2020). Desalination to remove electrolytes has been the mainstay of interventive conservation treatments for over a century yet its effectiveness has long been questioned. Determining an end point for desalination treatments involves monitoring chloride release; when outward diffusion of chloride ceases, measured as concentration of chloride in the wash bath, this is considered a proxy measurement

that all chloride is removed. To be successful, desalination will need to remove all soluble chlorides, adsorbed chloride from βFeOOH and access deep seated chloride beneath corrosion layers and in pits. This has not been shown to be successful, as chloride is detected within archaeological iron post-treatment (Rimmer et al. 2012). While this may be occluded in the βFeOOH where it does not support iron corrosion, anecdotal reporting of post treatment instability of washed iron and detection of large quantities of fresh βFeOOH on fragmenting objects, indicates not all chloride remains in this inaccessible form. Following desalination, it is realistic to expect iron to remain unstable but have enhanced stability compared to its untreated state and to corrode at a significantly slower rate.

Impact of βFeOOH on the corrosion rate of iron

Initial research used βFeOOH, produced by solid-state synthesis involving mixing iron powder with $FeCl_2 4H_2O$ at 92% RH, to investigate its impact on the corrosion rate of iron at low humidity (12%-35%) (Watkinson and Lewis 2005). Since oxidation of iron was recorded by mass gain, which records both oxidation and hydration, this prevented production of an oxidation rate graph. A remote sensing technique for quantitative measurement of oxygen concentration in a body of air (Matthiesen 2007; Matthiesen and Wonsyld 2010) has been adopted to provide a standardised reproducible experimental design for determining oxygen within an enclosed volume of air (Emmerson et al. 2021). This has been used to study the impact of washing on synthesised βFeOOH (Watkinson and Emmerson 2016) and corrosion rates of archaeological iron as a function of ambient RH (Watkinson et al. 2016; Watkinson et al. 2019) and is utilised in this study.

The data generated when using synthesised βFeOOH to study corrosion rates is likely to be influenced by the synthesis process. Solid-state (Turgoose 1982b) and precipitation (Mackay 1962; Reguer et al. 2009) methods are reported synthesis routes but each can be expected to produce varied chloride content, crystal shape and size in the end product. Crystal morphology influences the amount of surface adsorbed chloride, as does washing to refine the synthesis product, although this may not always be carried out. Amounts of occluded chloride can also vary. Post-synthesis purification washing may be either aqueous or anhydrous and it aims to remove excess reactants, specifically chloride compounds. Both the solvent used and the number of washes will influence the amount of adsorbed chloride on βFeOOH, which is normally reported as a mass percentage (mass%) of the βFeOOH.

Aim:

- To compare how differing βFeOOH synthesis methods influence its impact on the corrosion rate of iron and consider how this informs understanding of post-excavation corrosion and treatment of archaeological iron.

Objectives:

- Synthesise βFeOOH by solid-state and precipitation techniques, then wash these in cold water.
- Record the oxidation rate of iron mixed with synthesised βFeOOH using oxygen consumption and relate this to mass% of chloride removed during the wash process.

Method

βFeOOH was prepared either by precipitation or solid-state synthesis (Table 1). These were either past and newly synthesised samples with the synthesis year recorded in the sample labelling. Solid state βFeOOH production involved oxidising an iron powder/$FeCl_2 4H_2O$ mixture at 92% RH within a closed container. Danger of depleting oxygen to the point where magnetite (Fe_3O_4) is the thermodynamically favoured product was avoided by periodically facilitating oxygen ingress to the container.

Sample-synthesis year	Synthesis method	Post-synthesis washing
(P1-2021)	**Precipitation from solution** 3 L of 0.1M $FeCl_3 6H_2O$ solution in deionised water heated to 70°C for 48 hours. Filtered in Buchner funnel under vacuum. Rinsed with acetone x3. Ground with pestle and mortar for 10 minutes.	Acetone
(P2-2021)		
(S1-1983)	**Solid-state transformation** Iron powder (99.0% pure) mixed with equal mass $FeCl_2 4H_2O$ spread in petri dish enclosed in desiccator with beaker containing saturated solution of Na_2CO_3 to produce 92% ±5 RH.	Acetone
(S2-2000)	**Solid-state transformation** 25 g iron powder (Aldrich GPR™ 99.0% pure) mixed with 25 g $FeCl_2 4H_2O$ (BDH Chemicals 99.0% pure) spread in petri dish enclosed in desiccator with beaker	None

	containing saturated solution of Na_2CO_3 to produce 92% ±5 RH. No post-synthesis washing.	
(S3-2014)	**Solid-state transformation** 100 g iron powder (Aldrich GPR™ 99.0% pure) mixed with 100 g $FeCl_2 4H_2O$ (Sigma $\geq$ 99% pure) spread in petri dish enclosed in desiccator with beaker containing saturated solution of Na_2CO_3 to produce 92% ±5 RH. Humidity cabinet aerated regularly to ingress oxygen for 4 months. Residual $FeCl_2 4H_2O$ washed off with acetone using a Buchner funnel. Wash volumes unknown. NB for solid-state: Desiccator opened for short period of time daily to ingress oxygen over unspecified period of months. This avoids danger of depleting oxygen to the point where magnetite (Fe_3O_4) is the thermodynamically favoured product.	Acetone

Table 1. Synthesis methods for βFeOOH samples used in experimental work

For all βFeOOH samples, synthesis products were identified immediately prior to this experimental study, using a PANalytical X'Pert Pro (CuKα) X-ray powder diffractometer (XRD) and the data was interpreted using PANalytical X'Pert HighScore software. Imaging of βFeOOH crystals was carried out using a CamScan Maxim 2040 scanning electron microscope (SEM) equipped with Oxford Instruments energy dispersive X-ray spectrometer using secondary electron imaging. All

βFeOOH sample mass was recorded using a Sartorius Secura 225D-1S balance (readability 0.01 mg). Washing involved placing 0.05g of each sample individually in beakers and adding 10ml of deionised water then stirring continuously for 2 hours at room temperature. This will not remove all adsorbed chloride but offers a guide to the amount of chloride available for corrosion processes on each βFeOOH sample. Using a Microman® CP M1000E pipette, 500 µL (5 µL max systematic error and 3 µL max random error) sample solution was removed from each wash sample solution and chloride concentration was measured using a Sherwood Model 926 MKIII Industrial Chloride Analyser (accuracy: ±3 mg/L at 200 mg/L). This was scaled up to determine the βFeOOH mass% chloride for each synthesis method. The reproducibility of the analyser was measured using 177 ppm NaCl solution, before and after measuring a sample. Each solution was sampled three times for reproducibility.

To measure the impact of βFeOOH on the oxidation rate of iron, 0.05g of synthesised βFeOOH was mixed with 0.05 g of GPR™ iron powder, ground for 1 minute in an agate mortar then transferred to a plastic weigh boat that was placed in a Mason Ball reaction vessel with an airtight screw top lid, containing an oxygen sensor spot and 160 g of silica gel preconditioned to 80% RH (Emmerson et al. 2021). Since this was to be a comparative rate test, choosing a single fixed RH facilitates comparing rate between the various βFeOOH powders and 80% produces results quickly. This was placed in a Binder KBF720 climatic chamber controlled to 50%RH and 20ºC. A fibre optic cable attached to a PreSens Oxy-1 SMA oxygen was fixed to a support and placed against the Ruthenium sensor spot and fluorescence of the spot was recorded every 5 minutes in the dark interior of the climatic chamber

(Emmerson et al. 2021). Quenching of fluorescence is proportional to oxygen pressure in the reaction vessel.

Results and Discussion

Composition

XRD confirmed the samples as comprising only βFeOOH except for S2-2000, which contained a small amount of iron oxide hydroxide (αFeOOH) Reference Pattern: 01-076-7158 5 (Figure 1; Table 2). Where there are mixtures of compounds and fluorescence, detection limits are high potentially 15%. The βFeOOH match in all cases was Reference Pattern: 00-042-1315.

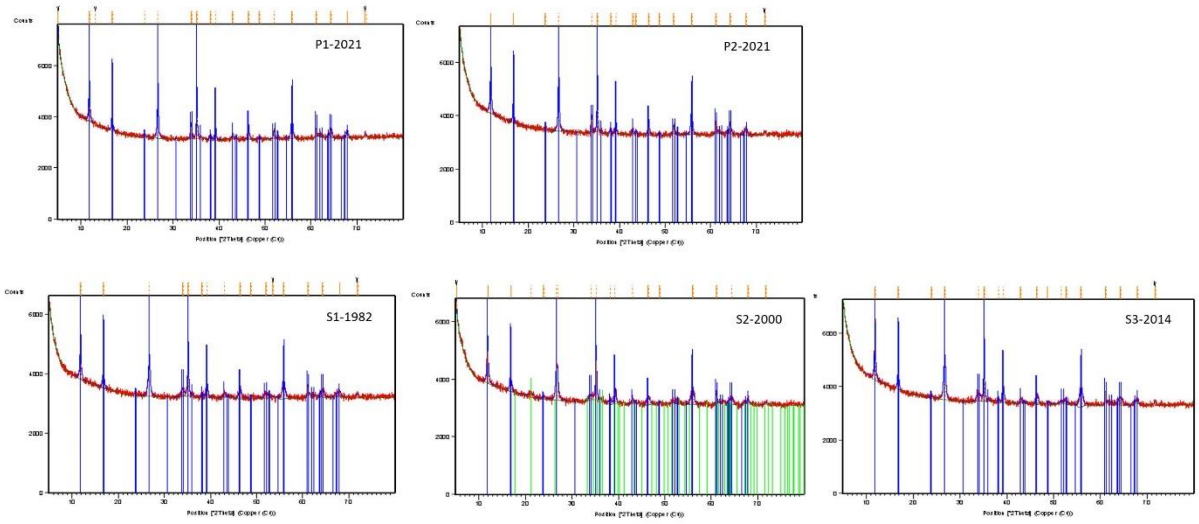

Figure 1. βFeOOH samples: X-ray diffraction data; left to right - Top P1-2021, P2-2021; Centre; S1-1983, S2-2000; Bottom; S3-2014.

Sample	XRD	Washing extraction (mass %)
P1-2021	Reference Pattern: 00-042-1315 Iron Oxide Chloride	1.5%

	Empirical Formula: $Cl_{1.3}Fe_8H_{9.7}O_{16}$	
P2-2021	Reference Pattern: 00-042-1315 Iron Oxide Chloride	2.0%
S1-1983	Reference Pattern: 00-042-1315 Iron Oxide Chloride	2.6%
S2-2000	Reference Pattern: 00-042-1315 Iron Oxide Chloride. Reference Pattern: 01-076-7158 5 Iron Oxide Hydroxide FeO(OH)	5.9%
S3-2014	00-042-1315 Iron Oxide Chloride	3.7%

Table 2. X-ray diffraction data and mass percentage chloride removed by washing in cold deionised water.

The βFeOOH samples were synthesised at differing times over a 38-year period (Table 1) and were later stored either sealed screw top glass jars, except for S1-1982, which was in a clip top plastic container. XRD performed in 2021 confirmed all samples contained βFeOOH and S2-2000 included an undermined amount of αFeOOH, which is a change from its original XRD data collected in 2000 when it was identified as being solely βFeOOH (Table 2; Figure 1). Gilberg and Seeley (1981) report thermodynamic instability of βFeOOH relative to αFeOOH but cite no examples. Thickett and Odlyha (2013) report atmospheric transformation of synthesised βFeOOH to αFeOOH occurring over a 6-month period, with higher RH producing more transformation and the presence of ethanoic acid vapour also promoting transformation. They detected similar transformations on βFeOOH samples formed on archaeological iron on display in showcases. The cause of the

XRD assay discrepancy for S2-2000 between the year 2000 and 2021 cannot be readily evidenced. Time cannot account for it as the older S1-1983 sample comprised only βFeOOH at its time of synthesis and has remained so, although S2-2000 differs in that it was not washed to purify it post-synthesis (Watkinson and Lewis 2005). Potentially, post synthesis environment and procedures for washing post-synthesis may have influenced transformation.

Unwashed βFeOOH has already been shown to corrode iron (Turgoose 1982b; Watkinson and Lewis 2005; Thickett and Oldyha 2013) and its transformation will increase its ability to corrode iron by releasing chloride from within its crystal structure. Similarly, if βFeOOH on archaeological iron has had its adsorbed chloride mostly or entirely removed by desalination treatments, transformation would reactivate its corrosion threat by releasing residual occluded chloride. At present, the transformation of corrosion products on washed archaeological iron seems to have not been studied.

Crystal structure and adsorbed chloride

Precipitated βFeOOH (P1-2021) produced smaller and more rounded crystal clusters compared with the larger and more elongated crystals in the solid state synthesis samples (S1-1982), S-2000, S3-2014) (Figure 2). This outcome tends to align with reported shapes and comparative sizes of crystals for precipitated and archaeological samples. Somatoidal crystals have been reported for the exact same precipitation synthesis (Garciua et. al. 2004) and Bayle et al. (2016) identified 0.5 µm rice shaped crystals in their precipitated βFeOOH. While no crystal shape data is reported for solid-state synthesis used in the study reported here, Mackay (1962)

identified elongated crystals in naturally formed βFeOOH and showed overall that crystal shapes for βFeOOH differ according to synthesis method and time. Rod shaped 1 µm length rod shaped crystals were identified in archaeological βFeOOH, which formed post excavation by transformation of β-$Fe_2(OH)_3Cl$ on an iron bar from a marine context (Bayle et al. 2016). The shape of the βFeOOH crystals is important, since surface area influences adsorption of chloride.

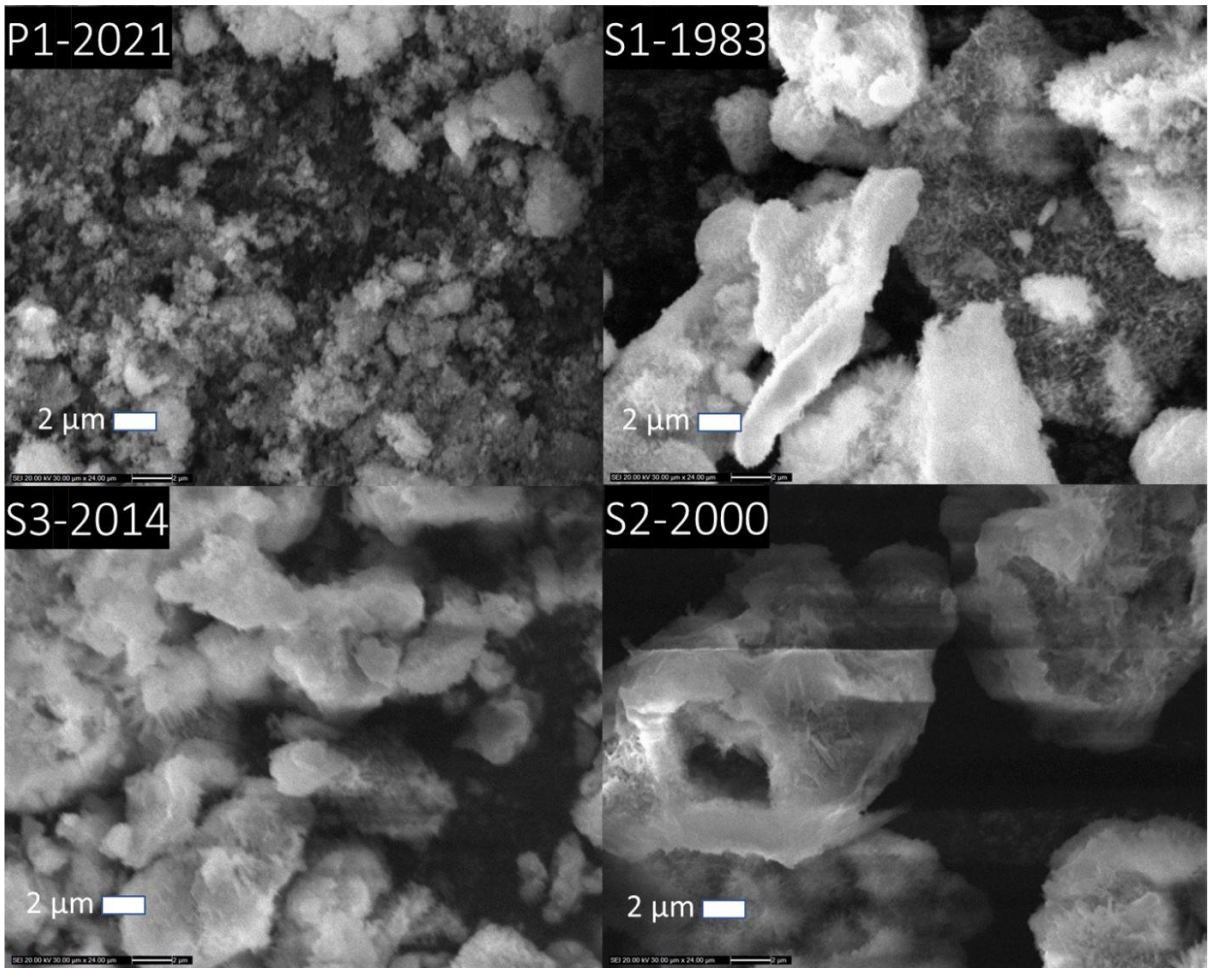

Figure 2. SEM images of the crystal structures of the βFeOOH samples synthesised by precipitation and solid-state reaction. Images 4000x magnification.

Adsorbed chloride on the βFeOOH, measured as the %mass chloride removed by the single cold water washing, ranges from 5.9% to 1.5%mass (Table 2). βFeOOH samples formed by precipitation have low mass% of surface adsorbed chloride, which differ (2 and 1.5 mass%) despite their similar synthesis (Table 1). As might be expected, due to it being unwashed following synthesis, S2-2000 has the most adsorbed chloride (5.9 mass%), while the acetone washed S1-1983 and S3-2014 have 2.6 and 3.7 mass% chloride respectively. Differences in crystal shape and/or acetone wash procedures could explain why the solid-state synthesised βFeOOH has more adsorbed chloride or for S2-2000 transformation to αFeOOH released occluded chloride.

The short wash time employed here has been shown to remove a significant amount of adsorbed chloride (Watkinson and Emmerson 2016). This identifies the high mobility of the adsorbed chloride and leads to the expectation that damp conditions will readily mobilise it, which is confirmed by the oxygen consumption corrosion rate tests carried out here (Figure 3). Once βFeOOH is cold water washed, its impact on the corrosion rate of iron falls significantly (Watkinson and Emmerson 2016).

Corrosion of iron by βFeOOH

Reaction of all the βFeOOH samples with iron, recorded as oxygen consumption, is initially fast (Figure 3), aided by the large surface area of the iron powder and mobility of adsorbed chloride at 80% RH. This creates an electrolyte at the interface between the iron powder and the βFeOOH, producing Fe^{2+} ions which hydrolyse, lowering the pH. According to the ratios of Fe^{2+} and Cl^- and the prevailing pH, βFeOOH will form; high concentration of Fe^{2+} and Cl^- favour production of only

βFeOOH, intermediate concentrations of Fe^{2+} favour αFeOOH; low Fe^{2+} concentration produces γFeOOH (Rémazeilles and Refait 2007). Mixtures of these compounds might be expected to occur in the corrosion formed here, since pH is expected to vary as Fe^{2+} is converted to corrosion products and hydrolysis is limited, also iron is depleted and the crusts of corrosion formed influence oxygen access to remaining iron particles, influencing oxygen access and consumption (Figure 3). Plotting the amount of adsorbed chloride removed from the βFeOOH by the cold water wash against the total amount of oxygen consumed by unwashed βFeOOH/iron powder mixtures over a 16-hour period, at which point reactions either cease or are significantly slowed, reveals a linear relationship (Figure 4). As might be expected, the greater the amount of adsorbed chloride the faster and more extensive the corrosion of the iron.

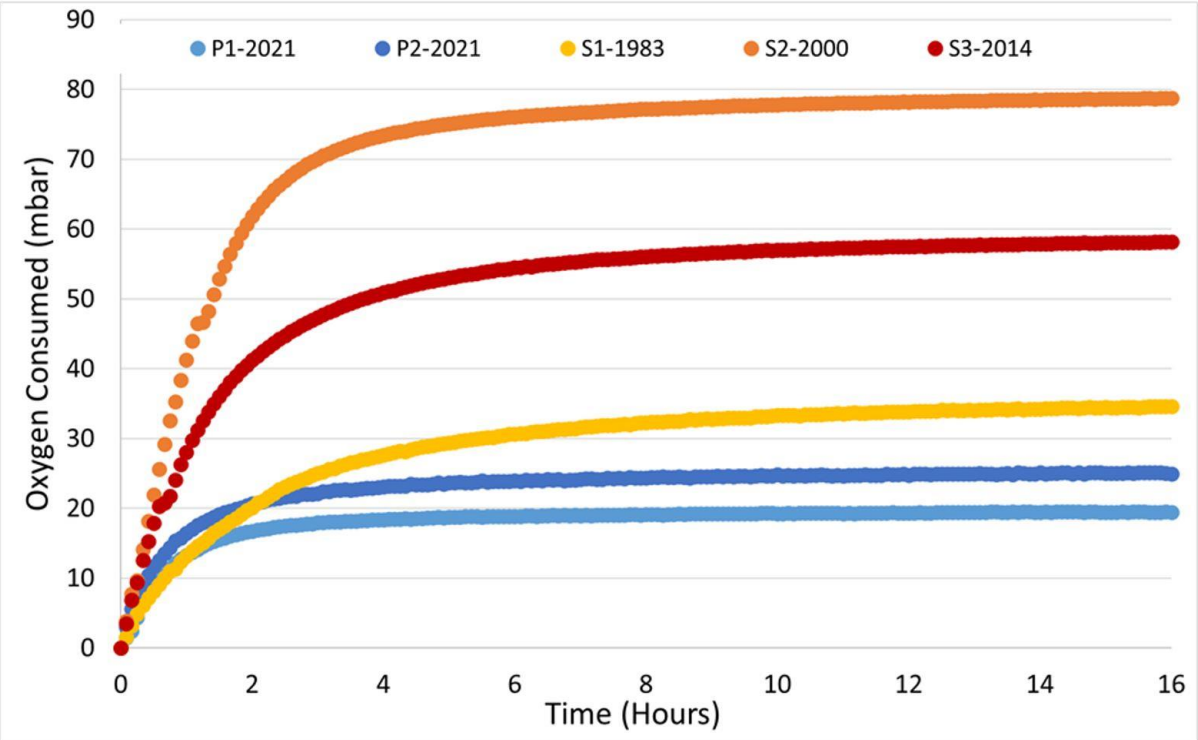

Figure 3. Oxygen consumption data for βFeOOH samples. Since the volume of all components of the reaction system in each case are identical, the mbar oxygen consumed can be used to compare rates within this sample set.

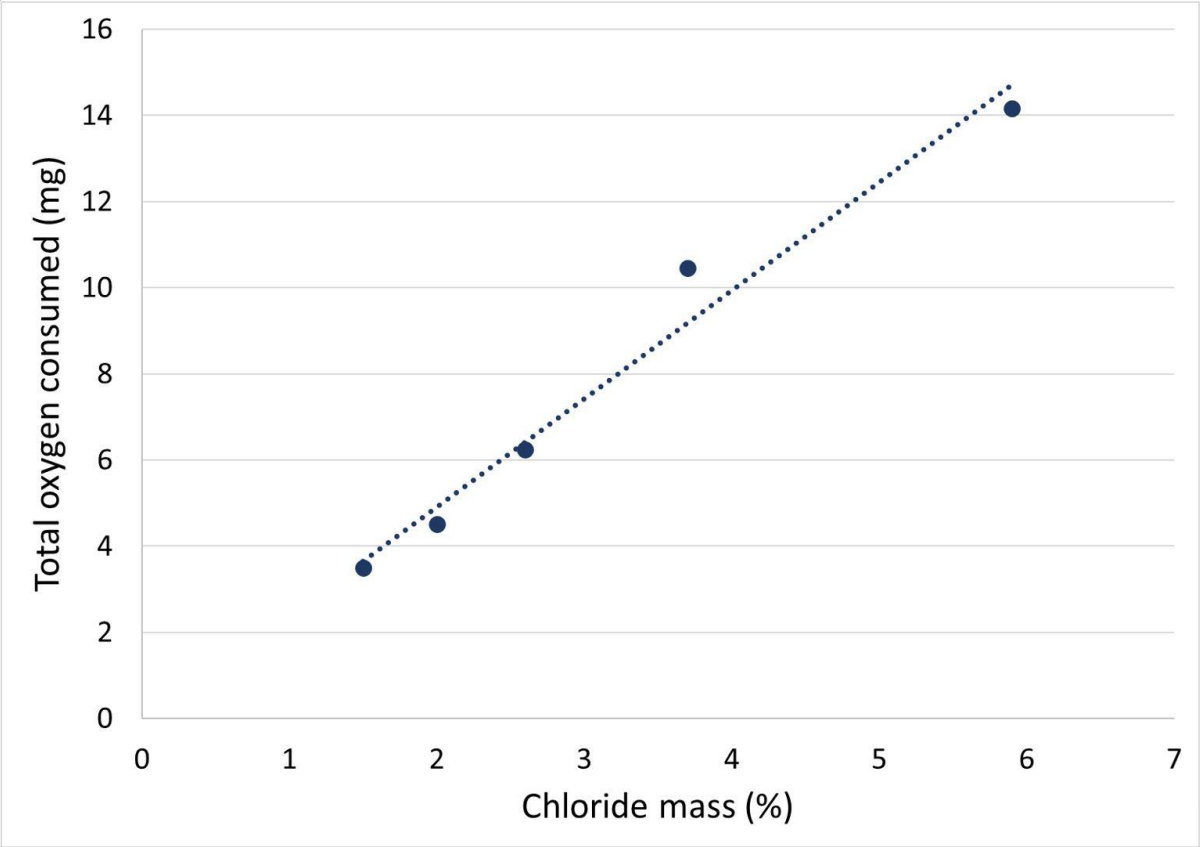

Figure 4. Oxygen consumed by βFeOOH/iron powder mixtures over the 16-hour logging time as a function of chloride removed by aqueous washing tests. (mbar converted to mg see Emmerson et al. 2021).

Context for conservation practice

When carrying out experimental studies using synthesised βFeOOH, extrapolating data quantitatively to archaeological iron contexts is challenging. Quantifying the risk of corrosion of archaeological iron as a rate factor of synthetic βFeOOH is not possible, as the amount of βFeOOH on objects, its adsorbed chloride mass and its accessibility to oxygen and moisture are all unknown. For investigating treatments aiming to remove adsorbed chloride from βFeOOH, using synthesised βFeOOH can offer insight into the impact of treatment parameters like solution composition,

concentration, temperature and time on chloride removal and βFeOOH transformation.

Conclusion

The corrosion risk to iron due to the presence of βFeOOH is a function of the mass of chloride adsorbed on the βFeOOH surface. This can differ appreciably according to the conditions in which βFeOOH forms and may change with time if transformations occur that release occluded chloride. Since solid-state formation routes are expected to occur on iron corroding in high humidity, the mass% of surface adsorbed chloride is likely to be high, as compared to βFeOOH formed from ionic solutions. In designing experimental studies using synthesised βFeOOH, its synthesis route should be taken into account when extrapolating results to practical contexts within conservation.

References

Bayle M., de Viviés P., Memet J.-B., Foy E., Dillmann P. and Neff D. 2016. Corrosion product transformations in alkaline baths under pressure and high temperature: The sub-critical stabilisation of marine iron artefacts stored under atmospheric conditions. Materials and corrosion, 67, No.2 190- 199.

Emmerson, N.J., Seifert, J.H and Watkinson, D.E. 2021. Refining the use of oxygen consumption as a proxy corrosion rate measure for archaeological and historic iron. *European Physical Journal Plus* 135.

Garcia, K.E., Morales, A.L., Barrero, C.A., Arroyave, C.E. and J.M. Greneche 2004. *Magnetic and crystal structure refinement in akaganeite nanoparticle*, Physica B 354:187–190.

Gilberg, M.R. and Seeley N.J. 1981. The identity of compounds containing chloride ions in marine iron corrosion products: a critical review. *Studies in Conservation* 26:50-6.

Mackay, A.L. 1962. β-Ferric oxyhydroxide—akaganéite. *Mineralogical magazine and journal of the Mineralogical Society,* Volume 3, Issue 259:270–280.

Matthiesen, H. 2007. A novel method to determine oxidation rates of heritage materials in vitro and in situ. *Studies in Conservation* 52:271–280.

Matthiesen, H. and Wonsyld, K. 2010. In situ measurement of oxygen consumption to estimate corrosion rates. *Corrosion Science Engineering and Technology* 45(5):350–356.

Neff, D., Vega, Dillmann. P. and Descotes, M. 2007. Contribution of iron archaeological artefacts to the estimation of average corrosion rates and the long-term corrosion mechanisms of low carbon steel. In Dillmann P., Beranger G., Piccardo P., Mathiesen H. (eds), *Corrosion of Metallic Heritage Artefacts: Investigation, Conservation and Prediction of Long-term Behaviour*; Woodhead: Cambridge, U.K. 41-74.

Reguer, S., Dillmann, P., Mirambet, F., Susini, J. and Lagarde, P. 2006. Investigation of Cl corrosion products of iron archaeological artefacts using micro-focused synchrotron X-ray absorption spectroscopy. *Applied Physics A –Materials Science & Processing* 83:189–193.

Reguer, S., Mirambet, F., Dooryhee, E. Hodeau J.-L., Dillmann, P. and Lagarde, P. 2009. Structural evidence for the desalination of akaganeite in the preservation of iron archaeological objects, using synchrotron X-ray powder diffraction and absorption spectroscopy. *Corrosion Science* 51:2795–2802.

Rémazeilles, C., and Refait, P. 2007. On the Formation of β- FeOOH (Akaganéite) in Chloride-Containing Environments. *Corrosion Science* 49:844–857.

Rimmer, M., Watkinson D. and Wang Q., 2012. The efficiency of chloride extraction from archaeological iron objects using deoxygenated alkaline solutions. *Studies in Conservation* 57:29-41.

Watkinson, D., Emmerson, N. and Seifert, J. 2017. Matching display relative humidity to corrosion rate: quantitative evidence for marine cast iron cannon balls. In R. Menon, C. Chemello, A. Pandya (ed.) Metal 2016 *Proceedings of the Interim Meeting of the ICOM-CC Metals Working Group September 26-30, 2016 New Delhi India*. ICOM-CC and IGNCA. 195-202.

Thickett, D. and Odlyha, M. 2013. The formation and transformation of akaganeite, in Metal 2013 Edinburgh, Scotland. Interim meeting of the international Council of

Museums Committee for Conservation Metal Working Group, E. Hyslop, V. Gonzalez, L. Troalen and L. Wilson, eds. Historic Scotland: Edinburgh, UK:103–109.

Thunberg, J., Watkinson, D. and Emmerson, N. 2021. Desiccated microclimates for heritage metals: creation and management. *Studies in Conservation* 66(3):127-153.

Turgoose, S. 1982a. The nature of surviving archaeological objects. In *Conservation of Iron*, Clark R. and Blackshaw S. (eds.) National Maritime Museum Monograph, 53:1-7.

Turgoose, S. 1982b. Post excavation changes in iron antiquities *Studies in Conservation* 27:97-101.

Watkinson, D. and Lewis, M. 2005. Desiccated storage of chloride contaminated archaeological iron objects. *Studies in Conservation* 50:241-252.

Watkinson, D. and Emmerson, N. 2016. The impact of aqueous washing on the ability of βFeOOH to corrode iron. *Journal Environmental Science and Pollution Research* 24 (3):2138–2149.

Watkinson, D.E., Rimmer, M.B. and Emmerson, N.J. 2019. The Influence of relative humidity and intrinsic chloride on post-excavation corrosion rates of archaeological wrought iron. *Studies in Conservation* 64:456-471.